Surface Wind Fields of 1995 Hurricanes Erin, Opal, Luis, Marilyn, and Roxanne at Landfall

MARK D. POWELL AND SAMUEL H. HOUSTON

NOAA/AOML Hurricane Research Division, Miami, Florida

ABSTRACT

Hurricanes Erin, Opal, Luis, Marilyn, and Roxanne were the most destructive hurricanes of 1995. At landfall, Luis and Marilyn contained maximum sustained winds (marine exposure) estimated at near 60 and 46 m s^{-1}, respectively. The strongest landfalling storm of the 1995 season, Luis, decreased in intensity from a category 4 to 3 on the Saffir–Simpson scale shortly before the eyewall crossed the Islands of Antigua, Barbuda, St. Kitts-Nevis, St. Barthelemy, St. Martin, and Anguilla. Hurricane Marilyn strengthened as it approached the U.S. Virgin Islands, with St. Thomas bearing the brunt of the north and south eyewall winds of 46 m s^{-1} (marine exposure) and St. Croix being affected by the relatively weak western eyewall peak winds of 35–40 m s^{-1} (marine exposure). For Luis and Marilyn only surface winds with marine exposures were analyzed because of unknown small-scale interactions associated with complex island terrain with 500–1000-m elevations. Wind engineering studies suggest that wind acceleration over blunt ridges can increase or "speed up" winds by 20%–80%. Topographic effects were evident in damage debris analyses and suggest that an operational method of assessing terrain-induced wind gusts (such as a scaled down mesoscale model) is needed. After landfall as a marginal hurricane over central Florida, Hurricane Erin regained strength over the Gulf of Mexico with a well-defined radar reflectivity structure. Erin struck the Florida panhandle near Navarre Beach with maximum sustained surface winds of 35–40 m s^{-1} affecting the Destin–Ft. Walton area. Hurricane Opal made landfall in nearly the identical area as Erin, with maximum sustained surface winds of 40–45 m s^{-1}, having weakened from an intensity of nearly 60 m s^{-1} only 10 h earlier. Opal was characterized by an asymmetric structure that was likely related to cold front interaction and an associated midlevel southwesterly jet. Roxanne struck Cozumel, Mexico, with sustained surface winds (marine exposure) of 46 s^{-1}, crossed the Yucatan, and meandered in the southwest Gulf of Mexico for several days. While in the Bay of Campeche, Roxanne's large area of hurricane-force winds disabled a vessel, which lead to the drowning deaths of five oil industry workers. High-resolution wind records are critical to preserving an accurate extreme wind climatology required for assessment of realistic building code risks. Unfortunately, power interruptions to Automated Surface Observing Stations on the U.S. Virgin Islands (St. Croix, St. Thomas) and Destin, Florida, prevented complete wind records of the eyewall passages of Marilyn and Opal, respectively.

1. Introduction

With the advent of modern distributed computing and rapid dissemination of data over networks, it is now feasible to analyze surface wind fields while a hurricane is in progress (Burpee et al. 1994). Real-time analyses assist hurricane forecasters in determining the location and extent of the strongest surface winds and help to identify locations experiencing the most severe winds and storm surge. Timely information on the actual areas impacted by a hurricane's eyewall and strongest winds should help to organize recovery management at the earliest stages following a disaster.

During the 1995 hurricane season the National Oceanic and Atmospheric Administration's (NOAA) Hurricane Research Division (HRD) produced 86 real-time analyses using techniques developed during the reconstruction of Hurricane Andrew's wind field (Powell et al. 1996; Powell and Houston 1996, hereafter referred to as PH). All available surface observations (e.g., ships, buoys, coastal platforms, surface aviation reports, reconnaissance aircraft data adjusted to the surface, etc.) are composited relative to the circulation center over a 4–6-h period of the storm's movement. All data are quality controlled and processed to conform to a common framework for height (10 m), exposure (marine or open terrain over land), and averaging period (maximum sustained 1-min wind speed) using accepted methods from micrometeorology and wind engineering. The analyses are made available to forecasters at the National Hurricane Center (NHC) on an experimental basis and poststorm analyses are conducted if sufficient new data become available.

While 1995 was the second most active Atlantic basin hurricane season on record, only 5 of the 19 storms caused significant loss of life and property. According

Corresponding author address: Dr. Mark D. Powell, NOAA Hurricane Research Division—AOML, 4301 Rickenbacker Causeway, Miami, FL 33149.
E-mail: powell@aoml.noaa.gov

to Lawrence et al. (1998), Hurricanes Luis, Marilyn, Erin, Opal, and Roxanne produced a combined damage total estimated at nearly $7.5 billion (U.S.), with 103 deaths. HRD conducted 49 real-time analyses in these storms (6 in Erin, 10 in Luis, 20 in Marilyn, 9 in Opal, and 4 in Roxanne) as indicated by the times and locations on the track charts presented in Figs. 1a and 1b. Sufficient poststorm data became available to justify reanalysis of Hurricanes Erin, Marilyn, and Opal at selected times. Hurricanes Luis and Marilyn were similar in that both affected islands with complex terrain that produced localized wind accelerations. Erin and Opal both hit the same area but were quite different in structure and resultant storm impact. This paper will document the surface wind fields of all five storms in the context of storm damage impacts, and extreme wind reports received from the public. Physical causes for asymmetries and intensity changes will be examined when warranted and warning lead times will be discussed.

2. Data and procedures

In most cases the primary data source is Air Force Reserves (AFRES) reconnaissance flight-level observations reduced from near 3 km to the surface with a boundary layer model (Powell 1980). For Hurricane Erin, 1500-m flight-level data were available. Flight-level wind speeds are assumed to be representative of mean boundary layer winds, although the 3-km level is above what is thought to be the boundary layer. The limitations of this approach are discussed in PH. Additional data sources include ships, NOAA National Data Buoy Center (NDBC) moored and drifting buoys, Coastal-Marine Automated Network (C-MAN) observations, surface airways (airport) observations including Automated Surface Observing Stations (ASOS), and a diverse set of supplemental data collected after landfall from additional public and private sources. Supplemental data for specific storms are discussed below. Data for a time period of 4–6 h undergo real-time and (when sufficient data are available) poststorm quality control before being sent to a nested, scale-controlled objective analysis package (Ooyama 1987; Lord and Franklin 1987; DeMaria et al. 1992). The resulting product is a streamline and isotach analysis representative of the maximum sustained (1-min average) wind field of the hurricane over the applicable time period. Most analyses are conducted for a marine exposure. If sufficient land observations are available, separate analyses are conducted for open terrain and merged with the marine analyses at the coastline. The merged analysis shows a discontinuity at the coastline associated with the transition of the flow from marine to land exposure (or vice versa).

In some cases, HRD analysis wind speed maxima will differ from NHC "best track" estimates described in the season summary (Lawrence et al. 1998). Differences
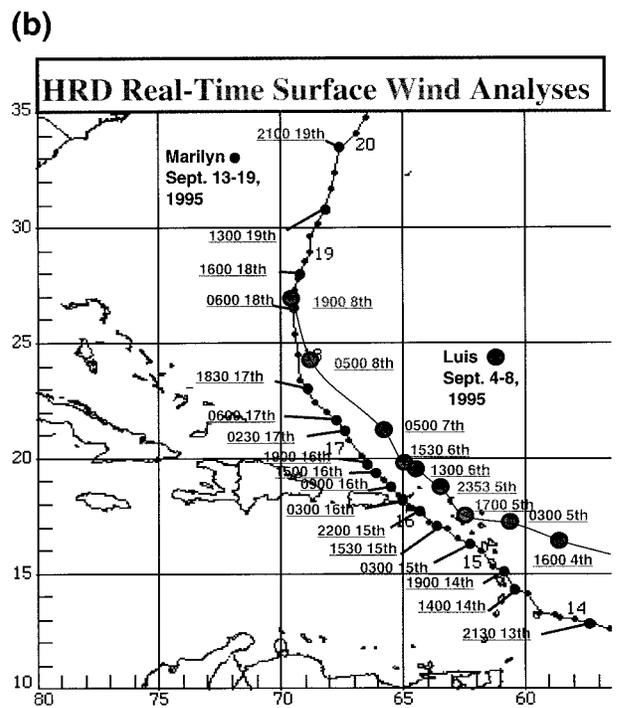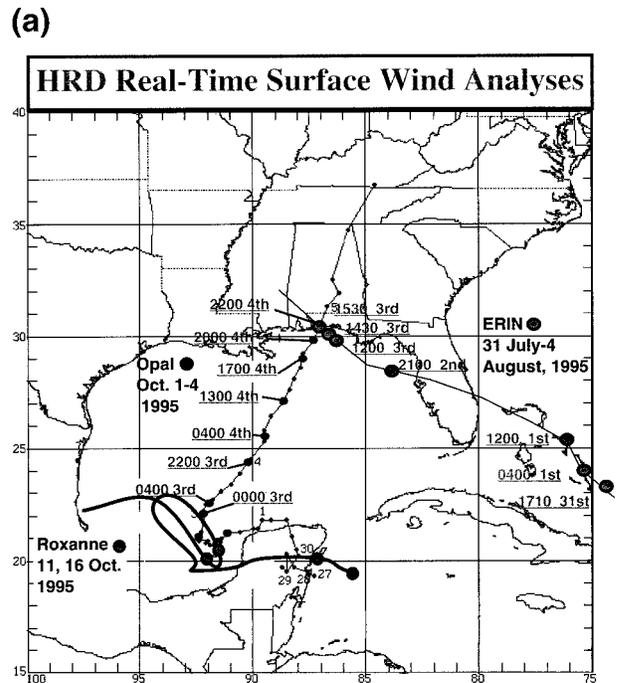
(a)

(b)

FIG. 1. HRD real-time surface wind analyses were conducted as indicated by the dates, times (UTC), and locations on the storm tracks for (a) Erin, Opal, and Roxanne and for (b) Luis and Marilyn.

during the 1995 season are associated with interpretation of the surface reduction of AFRES flight-level and WSR-88D Doppler wind velocity measurements. In addition to discussion of the reduction of aircraft wind measurements to the surface, PH describes a method for
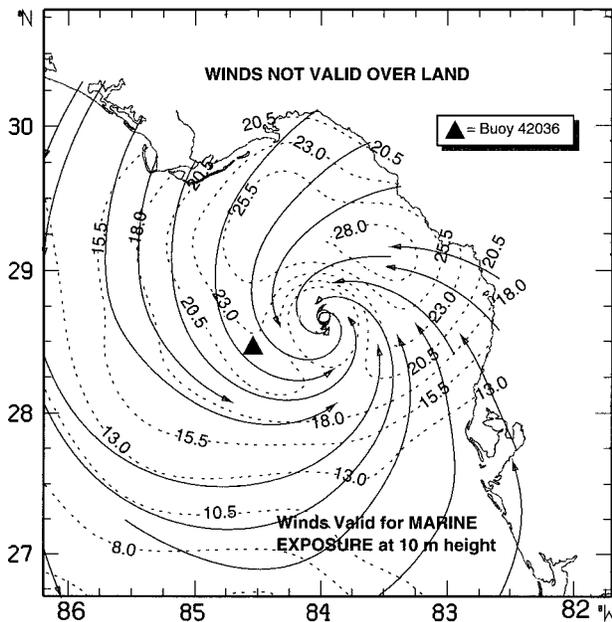
FIG. 2. HRD surface wind analysis for Tropical Storm Erin at 2100 UTC 2 August as it emerged over the Gulf of Mexico; streamlines and isotachs (m s^{-1}) are shown for marine exposure at 10-m height. The location of buoy 42036 is indicated.

inwardly repositioning surface-adjusted flight-level observations to account for the radial tilt of the eyewall. This method is not yet part of the real-time analysis system and is herein applied only to poststorm analyses conducted for Hurricanes Marilyn and Opal. Although HRD is conducting research on combining NOAA research aircraft and WSR-88D Doppler measurements and also working with other groups on developing WSR-88D algorithms for application to hurricanes (see http://www.nhc.noaa.gov/88dindex.html), only limited analyses of NOAA airborne Doppler radar velocity measurements collected in Hurricane Opal are presented in this paper. These analyses used the extended velocity track display algorithm (Roux and Marks 1996) to create three-dimensional wind fields from the 1- to 6-km altitudes over a domain of 150 km × 150 km centered on Hurricane Opal when it was offshore about 4 h before landfall.

3. Significant landfalls in the mainland United States

a. Hurricane Erin

Erin made its first United States landfall as a category 1 hurricane on the Saffir–Simpson scale (Saffir 1977; Simpson and Riehl 1981) near Vero Beach, Florida, at 0600 UTC 2 August 1995 (not shown). By 2100 UTC 2 August, Tropical Storm Erin emerged over the Gulf of Mexico (Fig. 2) with maximum sustained surface winds (V_{ms}) of 28 m s^{-1} about 60 km to the northeast of the circulation center. Data in this analysis included

AFRES observations adjusted to the surface from 1500 m (from 1725 to 2207 UTC) together with NDBC buoy observations from NOAA buoy 42036 and other marine surface observations from 1745 to 0200 UTC. This analysis confirms that Erin was still a tropical storm 2 h after the NHC issued a hurricane warning from the Suwanee River to the Pearl River (1900 UTC) and 2 h before the hurricane warning was extended westward to the mouth of the Mississippi River including New Orleans, Louisiana (2300 UTC).

Erin regained hurricane intensity near 0000 UTC 3 August and continued moving toward the west-northwest with the center making landfall in the vicinity of Pensacola, Florida, around 1600 UTC 3 August. A merged analysis wind field was constructed for the time that the highest V_{ms} winds would be affecting the coast at 1200 UTC. This analysis (Fig. 3) contains AFRES observations adjusted to the surface from the 1500-m flight-level (0957–1712 UTC) together with land and marine observations from 1000 to 1700 UTC. Maximum sustained surface winds of 39–41 m s^{-1} affected the marine exposed portions of Destin and Fort Walton Beach. Peak wind areas were associated with the eyewall as depicted by the overlay in Fig. 3 from the Eglin Air Force Base WSR-88D radar. Maximum sustained winds over land (open terrain) included 36 m s^{-1} (1409 UTC) from the Pensacola Regional Airport Federal Aviation Administration (FAA) Low-level Wind Shear Alert System, and 31 m s^{-1} at Eglin Air Force Base mesonet station B-71 (1444 UTC). The highest peak gust was 45 m s^{-1} measured at Pensacola Naval Air Station at 1600 UTC; severe weather associated with Erin included a tornado reported at Hurlburt Field (HRT) near the town of Mary Esther at 1330 UTC. The analysis in Fig. 3 was projected along the storm track to construct a V_{ms} swath (Fig. 4), which shows coastal winds in excess of 39 m s^{-1} from Destin to Pensacola Beach.

One concern of emergency management officials is the lead time for evacuation plans. Emergency managers plan evacuations and storm preparations according to a requirement that all activities must be completed by the onset of sustained gale force (18 m s^{-1}) winds. Here we define lead time as the period between the issuance of a hurricane warning and the onset of gale force winds. According to the observed track and wind analyses for marine and land (open terrain) exposure (not shown), gale force winds (marine exposure) would have begun along the coast near 0845 UTC, and inland (open terrain) around 1030 UTC, providing nearly 14 h of lead time for coastal areas and 15.5 h of lead time for areas just inland of the coast.

b. Hurricane Opal

Hurricane Opal struck the northwest Florida Gulf of Mexico coast on 4 October. According to Lawrence et al. (1998), Opal was a marginal category 3 hurricane at
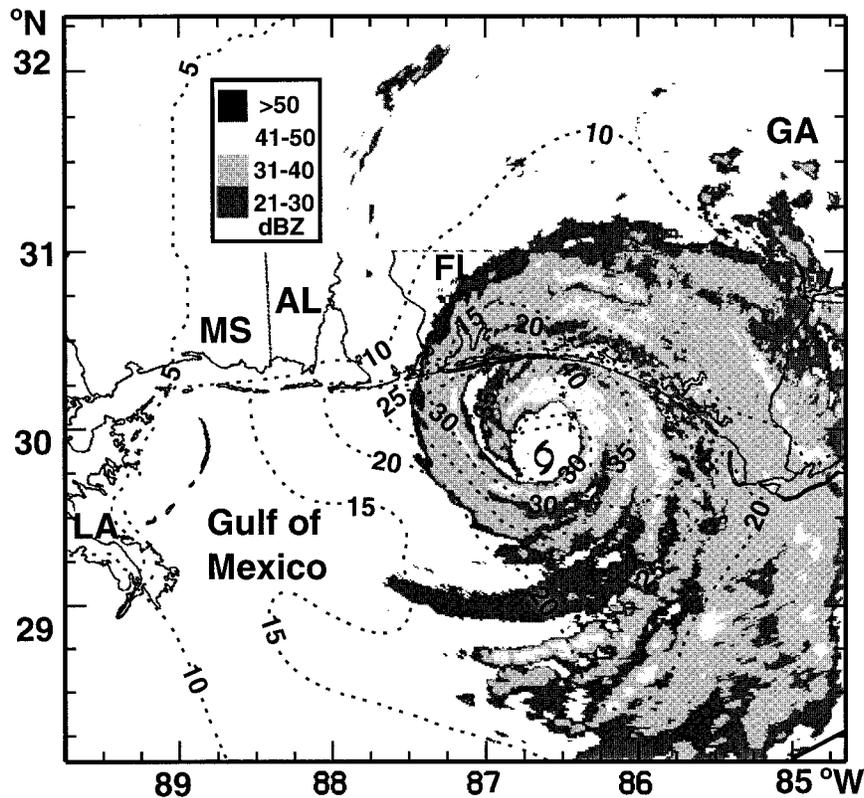
FIG. 3. Surface wind analysis for Hurricane Erin at 1200 UTC 3 August; isotachs (m s^{-1}) are shown for marine exposure over water and open-terrain exposure over land at 10-m height. Radar reflectivity data (dBZ) are shown for the Eglin AFB WSR-88D.

landfall. A combination of low central sea level pressure (SLP) at landfall of 94.2 kPa, storm surge estimated over 4.5 m, and waves (superimposed on the surge) of at least 3 m, contributed to Opal's categorization as a 3. Most of the affected area received winds of a category 1 or 2 hurricane, except for a small area from the extreme east end of Chochtawatchee Bay to about midway between Destin and Panama City Beach (Lawrence et al. 1998), based on AFRES measurements at 3 km and Doppler radar measurements from Eglin Air Force Base. HRD real-time analyses (not shown) indicated winds as high as 50 m s^{-1} in this area. After landfall, several additional data sources were collected from sites in the

Fig. 4. The analysis in Fig. 3 was projected along Erin's track to construct a V_{ms} swath according to the method described in PH.

vicinity of Baldwin County in Alabama, and Pensacola, Eglin Air Force Base, Panama City Beach, and Apalachicola in Florida. In addition, NOAA research aircraft Doppler radar measurements were analyzed.

Early on the day of landfall, Opal began to respond to an approaching midlatitude trough and increased its north-northeasterly speed from 6 to 10 m s^{-1}. This change in motion was accompanied by an intensification to category 4 status and an slp of 91.6 kPa in response to a combination of several possible factors including trough interaction, passage over the warm water of the Loop Current, and an eyewall contraction cycle (Willoughby et al. 1982). At this time, the HRD analysis (Fig. 5) for 1200 UTC 4 October suggests that Opal's peak V_{ms} winds were 59–62 m s^{-1} about 20 km to the east of the circulation center, with a secondary wind maximum of 51–54 m s^{-1} located about 60 km to the east of the center. Opal was characterized by an extremely asymmetric wind field structure with V_{ms} winds in the western eyewall reaching only 36–39 m s^{-1}. Data for the 1200 UTC analysis in Fig. 5 included selected AFRES observations from 0900 to 1312 UTC, NDBC buoy 42001 for 0525 to 1459, and additional marine observations from 0900 to 1500 UTC.
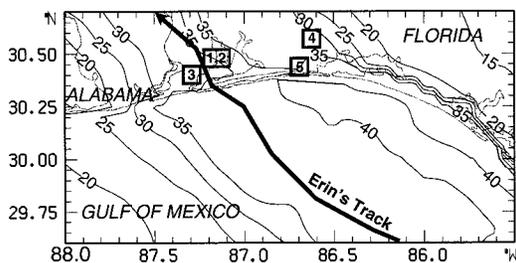
Fortunately, Opal began to weaken as the inner eyewall diminished and the outer, larger diameter eyewall
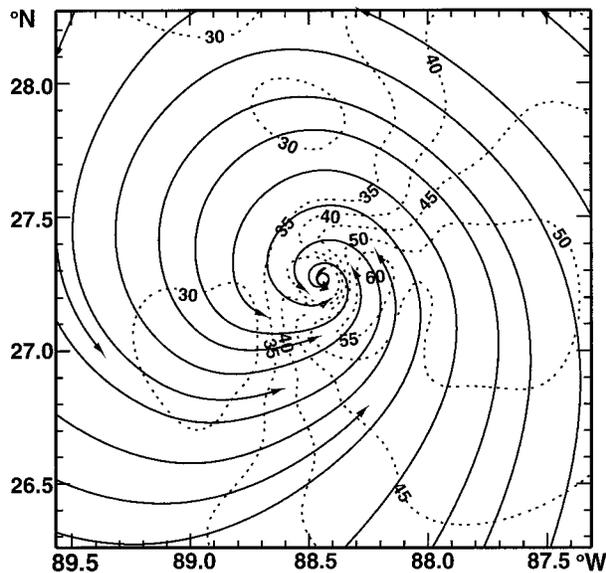
FIG. 5. Surface wind analysis for Hurricane Opal
at 1200 UTC 4 October.

became dominant. At the same time, Opal proceeded to interact with an approaching cold front while entering a region of lower sea surface temperatures in the northern Gulf of Mexico. Analysis of NOAA airborne Doppler measurements of the radial (relative to the storm) velocity component (Fig. 6) shows the influence of motion on the radial wind field and indicates that the affect of the cold front/midlatitude trough was to cause Opal to become embedded in a background flow from the southwest to northeast. This flow increased with height such that it was strongest at the 3-km level and well in excess of the storm motion. The effect of this type of flow would be to reinforce hurricane winds on the east side and diminish winds on the west side. Hence the height of maximum winds was 3 km on the east side and near 1 km on the west side. AFRES flight-level (3 km) winds on the west side of the storm were therefore weaker than nearby surface winds measured by C-MAN platforms at Dauphin Island, Alabama, and Southwest Pass, Louisiana, as Opal approached the coast.

Another factor affecting winds on the west side of Opal was the acceleration of the wind when passing from land to water. Offshore flow on the west side was relatively cool with air temperatures of 22°–24° C. When this air passed over the 27°–28°C water of the Gulf of Mexico, thermodynamically unstable conditions were created allowing vigorous mixing of higher momentum air from near 1 km. On the east side of the storm the flow was relatively warm; water temperatures were near or slightly cooler than the air causing slightly stable or neutral conditions with less mixing.

HRD conducted a postanalysis of Opal's wind field at landfall using only surface observations on the west side of the storm because the flight-level observations there were relatively weak. On the east side of the storm,

we used surface observations together with a limited amount of flight-level data where no surface information was available. As described in PH, flight-level measurements were assumed to be equivalent in magnitude to mean boundary layer winds and adjusted to the surface with a boundary layer model assuming neutral stability for oceanic exposure and stable conditions for open terrain roughness over land. Separate analyses were created in a storm-relative coordinate system for marine and land (open terrain) exposures. To help fill in data gaps and provide time continuity, a background field was created from an earlier analysis for 2115 UTC 4 October, which used data collected from 1616 to 2115 UTC. Background field grid points, ships, and adjusted aircraft data were weighted at 1%, 40%, and 70%, respectively, relative to the conventional surface observations (e.g., buoys, coastal platforms, airport anemometers, etc.). Both analyses used selected AFRES and marine and land surface observations from 2115 UTC 4 October to 0000 UTC 5 October. The analyses were then merged at the coastline resulting in Fig. 7. Merging the analyses creates a discontinuity at the coastline that represents a transition zone where the flow is adapting to a new underlying surface.

In the remnant eyewall to the northeast of the center V_{ms} winds of 45 m s^{-1} affected the area from Navarre Beach to Fort Walton Beach on the coast, decreasing to 35–40 m s^{-1} just inland. This maximum is based on a combination of observations from HRT, the Eglin Air Force Base mesonet, and adjusted air force reconnaissance flight-level observations. An isolated peak gust of 62 m s^{-1} was reported at the north end of HRT but the highest archived gust (3 km away at the south end of the runway) was 49 m s^{-1}, and it is uncertain whether the higher value was a result of the hot film anemometer system responding to cooling produced by rain or wind (a hot-film anemometer operates at a temperature near 100°C and measures wind by resistance changes due to cooling). Maximum winds extending east along the coast to the vicinity of Destin are based on adjusted flight-level measurements. This maximum is less prominent and located further west than the real-time analyses conducted during the storm because of the addition of NOAA National Ocean Service (NOS) observations from the Panama City Beach pier. Unfortunately, power was lost at the Destin (noncommissioned) ASOS station at 2119 UTC, preventing additional wind documentation. The peak wind before power loss was a V_{ms} of 26 m s^{-1} with a gust (5-s mean) to 33 m s^{-1}. Also noted in the analysis is the aforementioned increase of wind speeds on the west side of the storm due to enhanced turbulent mixing.

Projection of the 2140 UTC marine and land exposure wind fields along the forecast track suggest that gale force winds for marine exposure would have occurred along the coast about 1600 UTC, with gale force winds for open terrain exposure over land beginning near 1900 UTC. Given that a hurricane warning was issued at 0300

Hurricane Opal   1800 UTC 4 October 1995

NOAA Airborne Doppler radar analysis (plan view) of radial wind field at 3 km

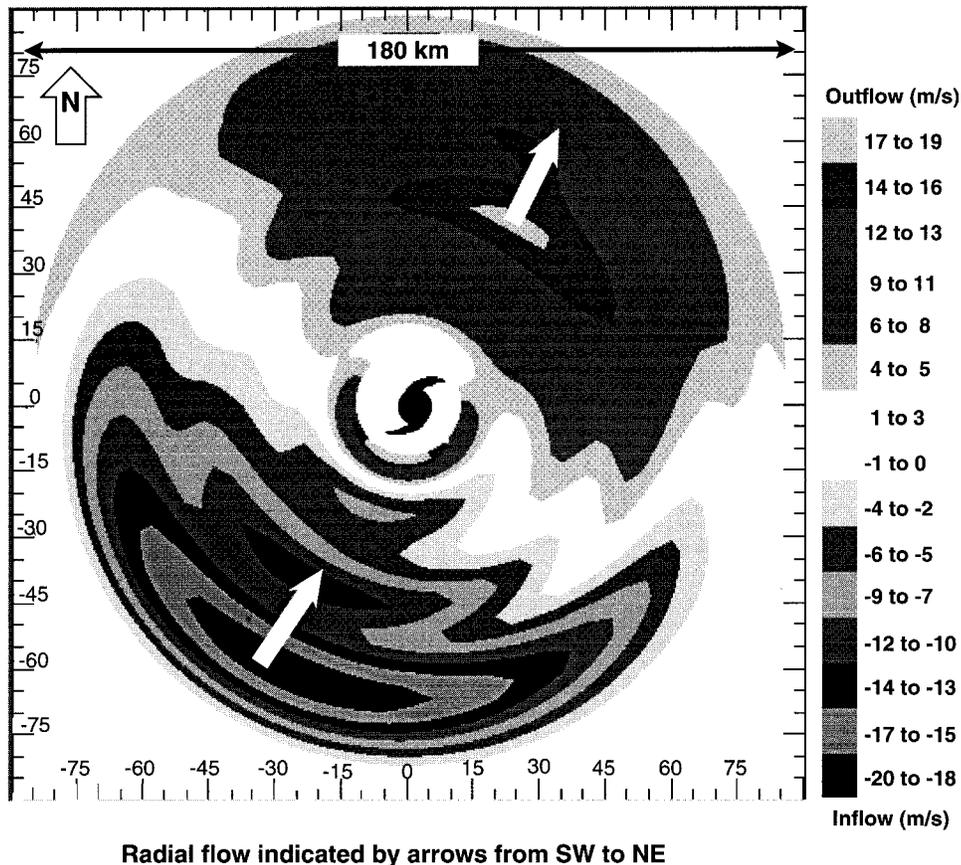**Radial flow indicated by arrows from SW to NE**

FIG. 6. Analysis of NOAA airborne Doppler measurements of the radial (relative to the storm) velocity component.

UTC 4 October (from Mobile, Alabama, to Anclote Key, Florida) this provided 13 h of lead time for the coast and 16 h for areas inland of the coast.

Another complication in the wind field may be related to the level of convective activity in the storm. At landfall (Fig. 7) most of the active convection was associated with the remnants of the northern eyewall; both airborne and WSR-88D radar indicated that no strong convection was visible to define the southern half of the eye. Typically, higher gusts are expected where convection is present. An outer rainband was located farther to the east where the flight-level winds measured by the air force reconnaissance aircraft were highest. According to NOAA aircraft radar observations from 5-km altitude, this band was not as convectively active as the remnant northern eyewall. The weaker convective activity of the outer rainband together with relatively stable or neutral air–sea temperature differences on the east side of the storm may have inhibited mixing of strong winds from the 3-km level to the surface.

A swath of the maximum sustained surface winds was constructed using the method described in PH; the swath field displayed in Fig. 8 illustrates the areas receiving the highest winds during Opal based on data collected through 15 December 1995. Again, the discontinuity at the coastline is consistent with a transition zone where the flow responds to a new underlying surface. The over-water portion of the swath depicts a broad 85-km-wide area on the east side of the storm with winds in excess of 44 m s^{-1}. Over land two wind maxima are apparent: one with winds over 41 m s^{-1} associated with the con-vective remnants of the eyewall about 30 km from the track, and one with 39 m s^{-1} winds about 80 km east of the storm track, related to an outer rainband.

Opal's weakening before landfall helped to minimize wind-related damage but the near-perpendicular track, coastline shape, large extent of hurricane force winds, and offshore bottom topography conspired to cause a high storm surge with superimposed waves that caused massive destruction to near shore structures as well as
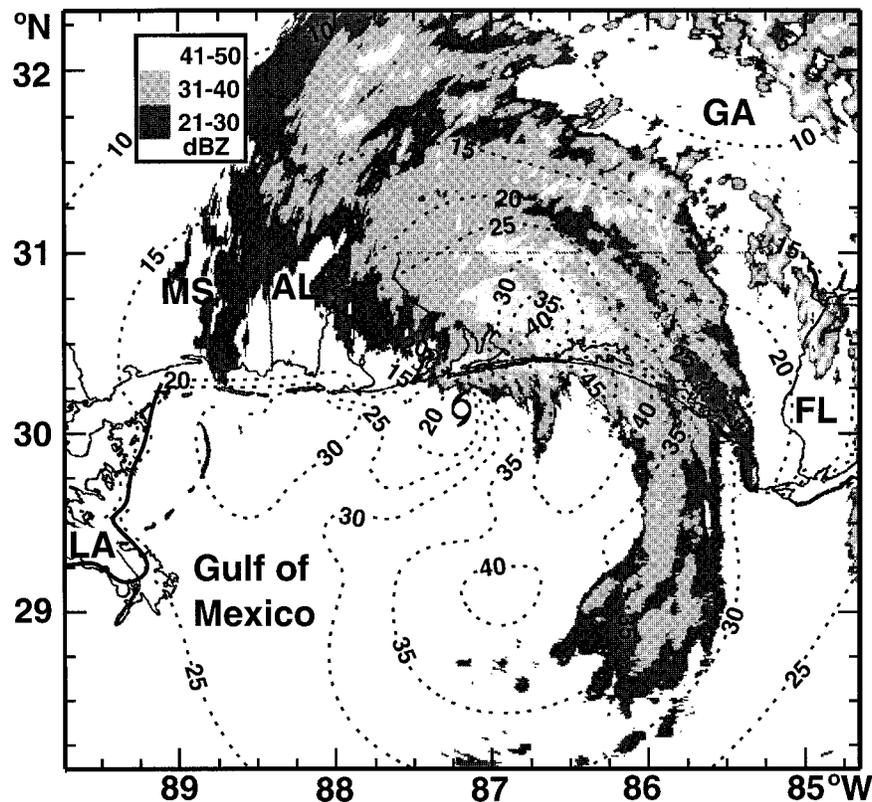
Fig. 7. Same as Fig. 3 except for Hurricane Opal at 2140 UTC 4 October.

coastal erosion from Pensacola Beach as far east as Apalachee Bay. Only one death (due to a tornado) was associated with Opal near the time of landfall. After landfall, eight deaths were attributed falling trees in Alabama, Georgia, and North Carolina as Opal gradually decayed inland.

In comparison, Hurricane Erin caused wind damage in the Pensacola Beach and Navarre Beach communities but little storm surge and wave damage compared to Opal. WSR-88D radar reflectivity distributions for Opal and Erin can be compared in Figs. 3 and 7, respectively. Erin was much more symmetric with a well-defined eyewall on all sides compared to the partial eyewall confined to the north side of Opal. Opal's partial eyewall

Fig. 8. Same as Fig. 4 except for Hurricane Opal.

was associated with entrainment of cooler, drier air associated with a cold front. The relatively small area of high reflectivity coverage in Opal's eyewall may have contributed to lower wind gusts and associated damages than might have been expected.

4. Significant landfalls in the Caribbean

a. Hurricane Luis

Hurricane Luis approached the Leeward Islands of the Caribbean as a category 4 storm on the Saffir–Simpson scale days before landfall. At 0300 UTC 5 September 1995, Luis (Fig. 9) contained maximum sustained surface winds (marine exposure) of 60–64 m s^{-1} in the northern eyewall about 60 km from the circulation center and hurricane force winds that extended over 200 km to the north and east. This analysis is based primarily on 70.0-kPa-level AFRES measurements (2232–0300 UTC) adjusted to the surface, and two ship observations at 2100 and 0000 UTC. The northwest and southeast eyewall of Luis passed directly over Barbuda with the southern eyewall affecting Antigua. Fortunately, Luis maintained an asymmetric structure with winds 10–15 m s^{-1} stronger on the north side than the south; the strongest winds likely passed offshore to the north of Barbuda. An observation of a 52 m s^{-1} maximum sus-
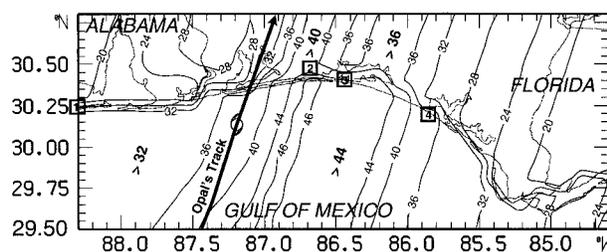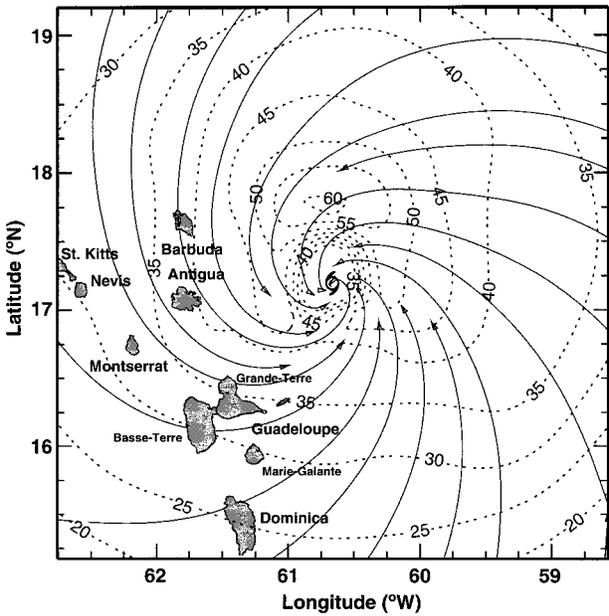
FIG. 9. Surface wind analysis for Hurricane Luis at 0300 UTC 5 September.
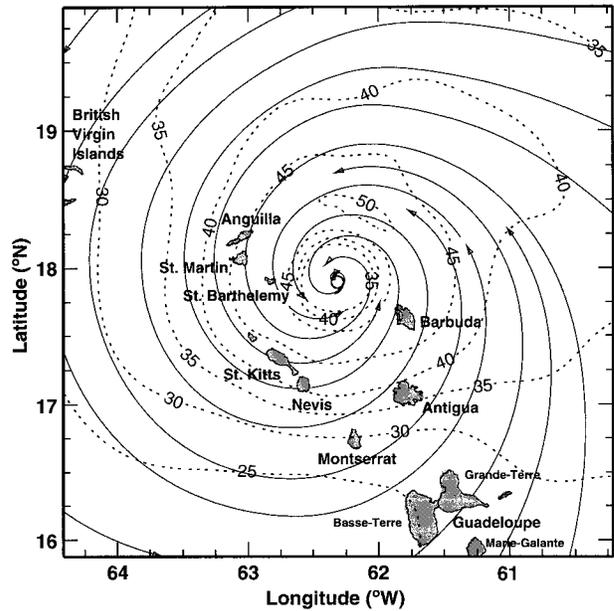

FIG. 10. Surface wind analysis for Hurricane Luis at 1700 UTC 5 September.

tained wind with a gust to 63 m s^{-1} reported at a United States–maintained air base on Antigua is slightly higher than analysis sustained winds that suggest a range of 45–50 m s^{-1} at that location, but the lead forecaster at Antigua mentioned that they were experiencing problems with their anemometer even before Luis (M. Mayfield 1995, personal communication). Earlier analyses (not shown) suggest that sustained gale force winds affected Antigua and Barbuda about 1000 UTC 4 September, providing about 10 h of lead time (hurricane warnings were issued at 0000 UTC 4 September).

By 1700 UTC 5 September Luis (Fig. 10) had weakened slightly with peak sustained winds (marine exposure) of 50–54 m s^{-1} located about 60 km north of the center. This analysis was based on 70.0-kPa-level AFRES winds from 1049 to 1551 UTC only. At this time the HRD analysis suggests that St Barthelemy, St. Martin, and Anguilla were affected by north and northwest winds of 45–50 m s^{-1} in the western eyewall. This is less than an observation of a 54 m s^{-1} maximum sustained wind with a gust to 67 m s^{-1} reported from St. Barthelemy (Lawrence et al. 1998). This difference may be due to local effects produced by mountainous terrain on the island or by the aircraft sampling winds at a level above the region of maximum winds.

b. Hurricane Marilyn

Hurricane Marilyn passed over Dominica and close to Martinique and Guadeloupe as a category 1 hurricane (not shown) on 14 September, and approached the U.S. Virgin Islands on 15 September as a category 2 (V_{ms}

43–49 m s^{-1}) storm as noted in the 1500 UTC public advisory. Marilyn's western eyewall passed over St. Croix around 2200 UTC 15 September (Fig. 11) with maximum sustained surface winds reaching 43–46 m s^{-1} about 25 km offshore to the northeast of the center. This analysis was based on 70.0-kPa-level, maximum 10-s wind AFRES observations collected at 30-s intervals from 1807 to 2031 UTC together with marine ob-
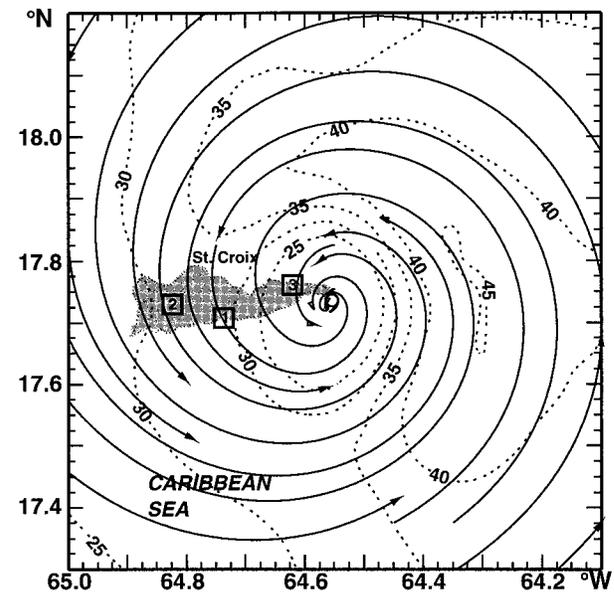

FIG. 11. Surface wind analysis for Hurricane Marilyn at 2200 UTC 15 September.

TABLE 1. Maximum 10-m wind speeds (m s^{-1}) in Hurricane Marilyn.

Locations (see numbers on analyses)	Time (UTC)	V_{ms} marine exposure based on Marshall and Schroeder (1997)	HRD analysis marine exposure
U.S. Virgin Islands			
1. St. Croix East Jetty	2324	41.4	39.4
2. St. Croix USDA	2315	40.5	39.5
3. St. Croix Green Cay Marina	Unknown	34.4*	34.3
4. St. Thomas ASOS	0532	43.2**	43.3

* Observation converted from gust to sustained wind.
** Higher winds of 51.6 m^{-1} (open terrain land exposure) occurred at 0352 UTC and may have been influenced by upstream topography. The HRD analysis showed 45.2 m s^{-1} winds (marine exposure) at this time.

servations from 1500 to 1800 UTC. Due to uncertainty about possible terrain affects on surface measurements, input data for HRD analyses of Marilyn were limited to AFRES winds adjusted to the surface with observation locations repositioned radially based on estimations of the location of the surface wind maximum using the (momentum surface tilt) method described in PH. The HRD analysis suggests that the highest sustained surface winds over St. Croix were caused by the northwest eyewall and reached 36–42 m s^{-1} over the eastern half of the island. Larger-scale analyses (not shown) indicated that gale force winds began on the southeast coast of St Croix about 1000 UTC 15 September. This provided approximately 13 h of lead time (hurricane warnings were issued at 2100 UTC 14 September) for emergency preparation activities.

Maximum (marine exposure) surface wind observations from Marshall and Schroeder (1997) are listed in Table 1. With the exception of observations from the

FIG. 12. Surface wind analysis for Hurricane Marilyn at 0330 UTC 16 September.

St. Thomas ASOS from 0517 to 0531 UTC, marine observations in Table 1 were not input to the HRD analysis. Most of these reports are close in magnitude to the HRD marine exposure winds of Fig. 11. Unfortunately power was cut off to a noncommissioned ASOS station on St. Croix when the Alexander Hamilton Airport was closed before the storm. The sailboat *Puffin,* moored at Green Cay Marina, measured a peak gust of 44 m s^{-1}, and anemometers at the Hess Oil refinery and the U.S. Department of Agriculture measured sustained 40.5 and 41.4 m s^{-1} winds, respectively, which are similar to the HRD analysis. An unconfirmed peak gust of 57 m s^{-1} at the eastern end of St. Croix was mentioned in the National Weather Service (NWS) disaster survey report (Wernly 1996). Using gust factors (Powell et al. 1991) for the ratio of a peak gust to a maximum sustained wind of 1.3 (for turbulent gusts) to 1.6 (for extreme convective gusts) yields an estimated sustained wind range of 35–44 m s^{-1}, which is consistent with the HRD marine exposure analysis. Marilyn had a much lower impact on St. Croix than Hurricane Hugo did in 1989; analysis of Hugo's passage over the island (National Research Council 1994) depicted maximum sustained winds of 57 m s^{-1}.

Marilyn continued northwestward with the northern eyewall striking St. Thomas and St. John near 0300 UTC 16 September (Fig. 12) with easterly V_{ms} (marine exposure) winds of 46 m s^{-1} located about 25 km from the circulation center. Observations used for this analysis included 70.0-kPa-level peak 10-s AFRES measurements from 0029 to 0330 and marine surface reports from 2300 to 0000 UTC. The Puerto Rican island of Culebra was just beginning to be affected by the northwest eyewall at this time. Gale force winds affected the islands of St. Thomas and St. John near 1630 UTC 15 September (a lead time of 19.5 h).

By 0438 UTC (Fig. 13), the eastern eyewall was over eastern St. Thomas and maximum marine-exposure winds increased to 48 m s^{-1} from the southeast about 22 km from the circulation center. Observations used for the 0438 UTC analysis included 70.0-kPa-level peak 10 s AFRES measurements from 0522 to 0838 UTC (which included the highest winds measured during
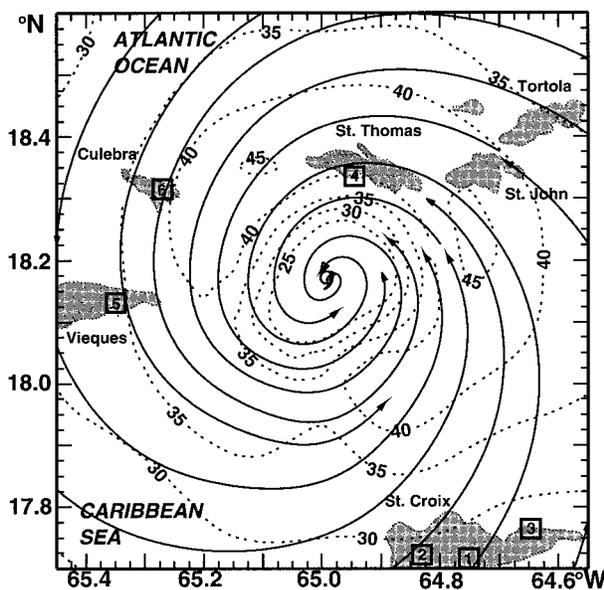
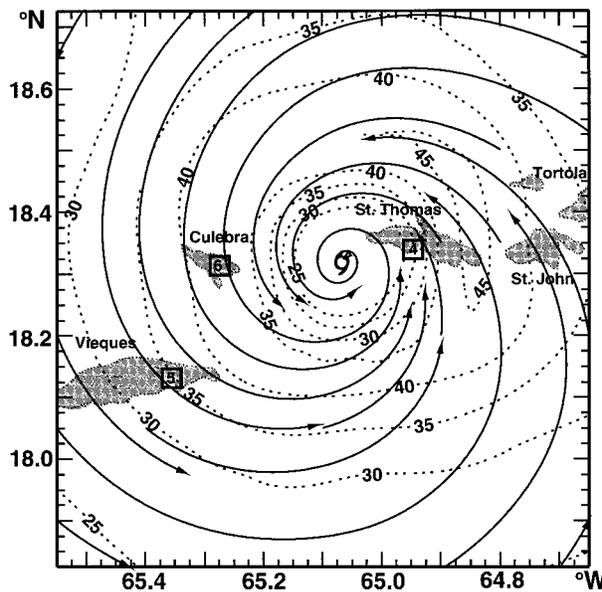FIG. 13. Surface wind analysis for Hurricane Marilyn at 0438 UTC 16 September.

FIG. 14. Same as Fig. 4 except for Hurricane Marilyn, numbers refer to wind observation locations in Table 1.

Marilyn's landfall) and marine-exposed ASOS observations from 0517 to 0531 UTC. At this time St. John was slightly outside the eyewall with 41–44 m s^{-1} winds from the southeast, Culebra's winds in the western eyewall were north-northwest at 39–44 m s^{-1} and the Puerto Rican island of Vieques was just outside the southwest eyewall with peak marine exposure winds of 33–38 m s^{-1} from the northwest. Noncommissioned ASOS data retrieved after the storm from St. Thomas' Cyril King Airport indicated that maximum (open terrain exposure) V_{ms} wind in the northern eyewall was 51.6 m s^{-1} from the northeast at 0352 UTC (17 km north of the circulation center) with a peak (5-s mean) gust of 58 m s^{-1} occurring at 0408 UTC (only 13 km from the center). At 0352 UTC, a 44.5 m s^{-1} V_{ms} from the HRD analysis was located 12 km radially outward from the ASOS location, despite efforts to correct the locations of maximum winds in the HRD analysis to account for the vertical tilt caused by thermal wind shear. Winds at the ASOS decreased to less than 15 m s^{-1} in the eye and then increased again reaching 43.2 m s^{-1} at 0532 UTC as the wind shifted onshore from the south in the southern eyewall. A power failure prevented further documentation of marine exposure winds.

A swath of Marilyn's maximum sustained winds is presented in Fig. 14 along with locations of confirmed wind reports listed in Table 1. Unconfirmed maximum wind reports with unknown time references (Wernly 1996) include a sustained wind of 67 m s^{-1} from the WVWI radio station antenna on St. Thomas, and an estimated wind of 76–78 m s^{-1} from the Virgin Islands Territorial Emergency Management Agency (VITEMA) at Susannaberg on St. Johns (Lohr 1995; Husty 1995).
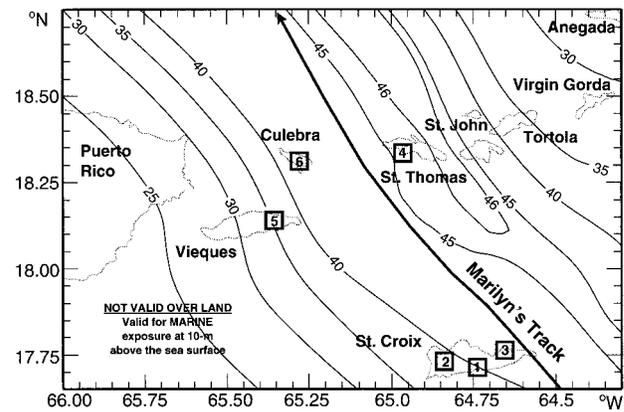
Sustained winds of the magnitude attributed to these two locations are highly unlikely since they would imply gusts of 87 and 100 m s^{-1}, respectively, the highest gusts ever recorded in hurricanes. If we consider that these reports may have been representative of peak gusts, application of gust factors suggests a range of sustained winds of 42–52 m s^{-1} at the radio station antenna and 47–60 m s^{-1} on St. Johns. Considering that eight locations of F2 damage debris (Wernly 1996) were found on St. Thomas compared to only F1 damage on St. John, the radio antenna observation (if we assume it was a gust) is plausible; the report for St. Johns appears too high even as a gust report unless very unusual terrain-enhanced accelerations were taking place. Additional undocumented reports (Wernly 1996) include an amateur radio report of 45 m s^{-1} sustained winds on Vieques at 0400 UTC, and a local emergency management report of sustained winds of 45 m s^{-1} on Culebra from 0500 to 0600 UTC. The reports from Culebra are slightly higher than the HRD analysis and the aerial survey of damage debris, while the report from Vieques appears too high in comparison with the HRD analysis and a report from the U.S. Geological Survey (USGS) station at Camp Garcia of 19.8 m s^{-1}. In comparison, analysis of Hurricane Hugo's passage over the same areas (National Research Council 1994) was associated with maximum sustained winds estimated at 54 m s^{-1} on Culebra, 49 m s^{-1} on Vieques, and 44 m s^{-1} on St. Thomas.

c. Topographic effects

Damage surveys of Hurricanes Hugo (National Research Council 1994), Iniki (Fujita 1993), and Marilyn (Wernly 1996) provide compelling evidence that structures exposed on hillsides and hilltops are more susceptible to wind damage than those located at lower elevations. A graphic of the NOAA nautical chart for St. Thomas is shown in Fig. 15 together with locations
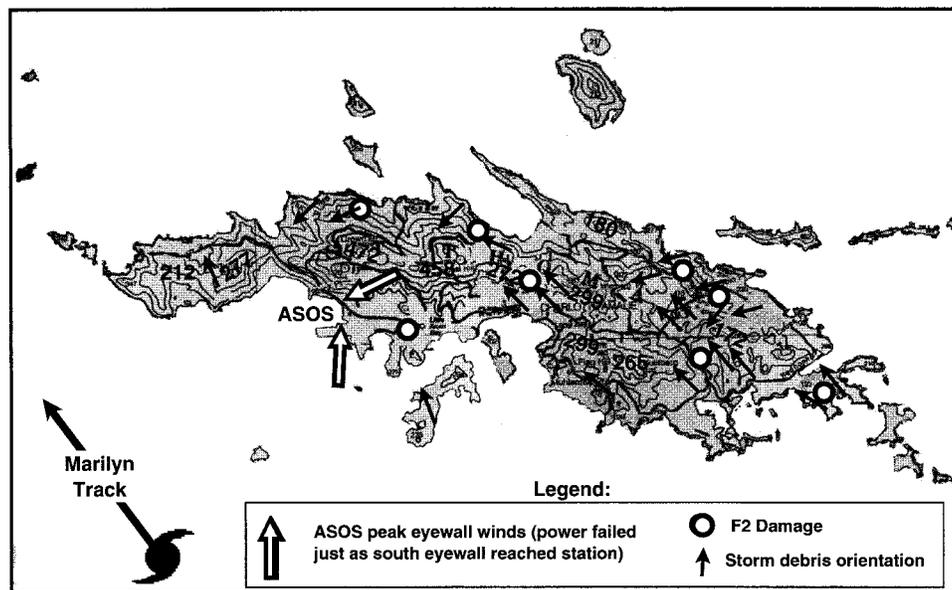
FIG. 15. NOAA nautical chart for St. Thomas showing elevation contours at 100-m increments; locations of extreme wind reports and locations of F2 damage and nearby debris distribution directions based on the damage debris survey of Marilyn (Wernly 1996).

of the ASOS station and F2 damage and nearby debris distribution directions based on the damage debris survey of Marilyn (Wernly 1996). Normally HRD studies of landfalling hurricanes include poststorm analysis of open exposure winds over land. In the case of mountainous coastal terrain, such analyses are unable to account for small-scale interactions between the wind and the elevation and shape of the topography. Hence, HRD wind analyses in regions with mountainous terrain maintain use of the "marine exposure" analysis. Since input data to the analysis system in these areas is primarily adjusted aircraft reconnaissance measurements and ships, the marine exposure analysis is more conservative (with higher wind speeds) than the open terrain analysis.

Studies of the influence of bluff bodies such as hills and escarpments on wind flow (Jackson and Hunt 1975; Jensen and Peterson 1978; Bradley 1980) suggest that flow accelerates near the crests of hills with a flow separation bubble extending downwind on the lee side. Field investigations of flow over bluff bodies have been limited to relatively low wind speeds [e.g., 22 m s^{-1} by Holmes et al. (1998)]. Wind tunnel studies (Glanville and Kwok 1998; Means et al. 1996) have compared well with full-scale field measurements and show similar acceleration and separation features in simulations with scaled winds in excess of hurricane force. According to Marshall and Schroeder (1997), these effects were integrated into the Caribbean Uniform Building Code (1989, hereafter CUBC). Wind load standards in Australia, Canada, and the United States also account for terrain affects on wind by using "speedup" factors or "topographic multipliers" (e.g., Standards Australia

1989; ASCE 1995). The wind speed at a given height above the hill is estimated by multiplying the upstream wind value (at the same height above level ground) by the speedup factor. For wind flow normal to a steep (0.25 gradient) 100-m-high ridge, CUBC (1989) uses a speedup factor of 1.8 at an elevation of 5 m above the surface of the hill. Unfortunately, according to Marshall and Schroeder (1997) the U.S. Virgin Islands were not under the jurisdiction of this code. If we apply such a speedup factor to a representative peak 10-min mean wind of 40 m s^{-1} over St. Thomas, we obtain hilltop winds as high as 74 m s^{-1}, which is close to the unconfirmed reports from WVWI and VITEMA on St. Johns. Flow over complex terrain is complicated by the shape and size of the terrain features. For example, Holmes et al. (1996) found topographic multipliers of 1.20 and high turbulent intensity at 32 m above an escarpment (within the separation zone) compared to a multiplier range of 1.73–1.95 and low turbulent intensity at 69-m elevation (outside the separation zone). High quality, high-resolution wind information on bluff bodies in hurricane winds is required to determine whether speedup factors such as those used in CUBC (1989) are representative. If the CUBC-type speedup factors are realistic over steep hill tops, even a marginal category 1 hurricane can contain winds of category 3 intensity, and a weak category 2 storm could produce category 5 winds. This is a serious concern that needs to be addressed in hurricane warnings and advisories for hilly or mountainous locations; it should also be addressed in building codes for such areas.

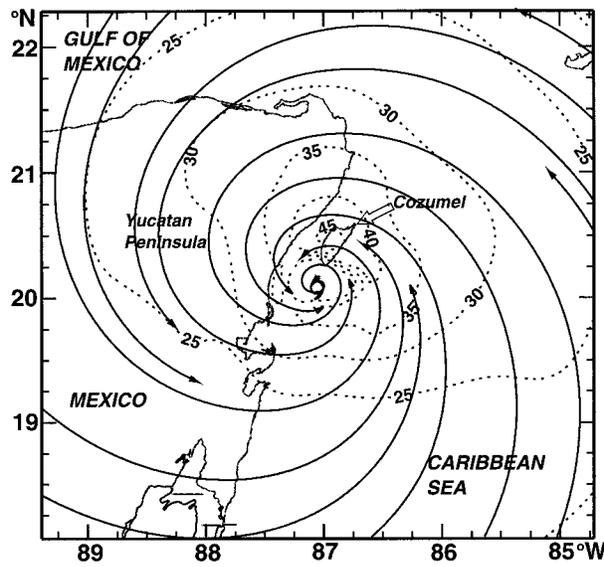Mesoscale atmospheric models may have the poten-

FIG. 16. Surface wind analysis for Hurricane Roxanne at
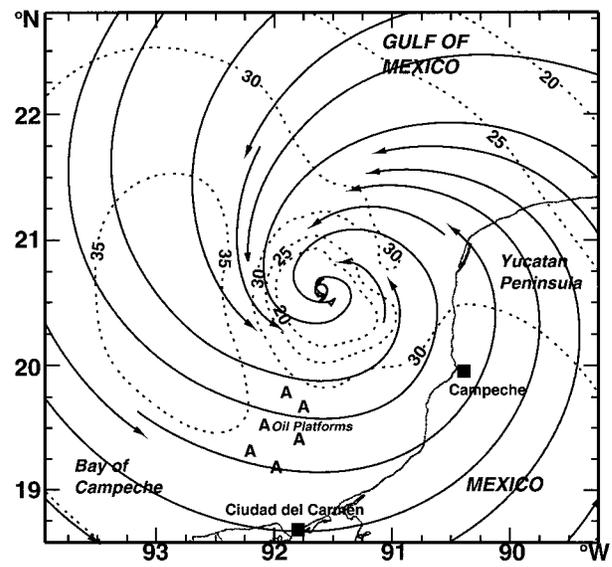0000 UTC 11 October.

FIG. 17. Surface wind analysis for Hurricane Roxanne at
1800 UTC 16 October.

tial to identify localized accelerations induced by terrain
provided that high-resolution topography is available.
To test this idea, Nicholls and Pielke (1996, personal
communication) are adapting the Regional Atmospheric
Modeling System to the terrain of St. Thomas to eval-
uate changes to a uniform hurricane-force wind field as
a function of wind direction. If this work is successful,
it is possible that the wind field of an approaching hur-
ricane could be input to a model to predict a range of
extreme winds possible over threatened islands and
identify locations susceptible to the wind hazard.

d. Hurricane Roxanne

Roxanne made landfall just south of Cozumel in the
Mexican state of Quintana Roo, near 0200 UTC 11 Oc-
tober 1995. The strongest V_{ms} marine exposure winds
of just over 46 m s^{-1} (Fig. 16) were located in the
northern eyewall, which passed directly over Cozumel
about 45 km from the circulation center. The analysis
in Fig. 16 was based on 70.0-kPa-level AFRES obser-
vations from 1813 to 2345 UTC together with marine
surface measurements from 1500 to 2100 UTC.

Roxanne continued across the Yucatan peninsula and
into the Gulf of Mexico where it meandered for several
days. Late on 15 October, Roxanne moved southward
toward the Bay of Campeche. Oil rigs in the area that
had been evacuated the previous week were being reoc-
cupied and at 2345 UTC 15 October, a barge sank
drowning 5 and forcing the rescue of 240 oil workers
offshore from Ciudad del Carmen, Mexico (Associated
Press 1995). At 1800 UTC 15 October, the HRD analysis
(Fig. 17) suggests that peak V_{ms} winds were 35 m s^{-1}
about 110 km to the west of the circulation center, and

that an extensive area of hurricane force winds extended
over 200 km outward from the center on the west side
of the storm. This analysis is based on 70.0-kPa-level
AFRES observations from 1221 to 1711 UTC together
with marine surface measurements from 1200 to 1500
UTC.

Roxanne became a hurricane at 0600 UTC 10 Sep-
tember, only 3 h after a hurricane warning had been
issued (0300 UTC). According to an HRD analysis po-
sitioned at 0300 UTC (based on AFRES data collected
from 1026 to 1330 UTC 10 September), the warning
was issued at roughly the same time that gale force
winds began (no lead time) but a tropical storm warning
and hurricane watch had been in affect since 2100 UTC
on 9 September (6-h lead time based on watch issuance).
Roxanne is a good example of the need to prepare for
hurricane conditions even when a tropical storm is im-
minent due to uncertainty in forecasting intensification.

5. Validity of the pressure–wind relationship

Pressure–wind (PW) relationships (e.g., Fujita 1971;
Atkinson and Holliday 1977; Dvorak 1984) are helpful
for estimating winds in the absence of observations and
have the form

$$V_{ms} = A[10(P_o - P_{min})]^b, \tag{1}$$

where P_o is the peripheral SLP (assumed to be 101.0
kPa), P_{min} is the minimum SLP (kPa), and A and b are
constants. For example, application of PW relationships
to Hurricane Opal at landfall results in V_{ms} winds of
52.5, 52.3, and 55.8 m s^{-1} using the relationships of
Atkinson and Holliday ($A = 3.45$, $b = 0.644$), Dvorak
($A = 3.4$ $b = 0.648$), and Fujita ($A = 4.89$, $b = 0.577$),

TABLE 2. Comparisons between HRD analysis and pressure–wind relationship wind speeds (m s^{-1}); Time—time (UTC) of HRD analysis, HRD—V_{ms} from HRD analysis, DelP—pressure deficit (kPa), D—Dvorak pressure–wind relationship, A&H—Atkinson and Holliday pressure–wind relationship, and F—Fujita pressure–wind relationship.

Storm	Time	Date	HRD	DelP	D	A&H	F
Erin	1200	3 Aug	41.0	3.6	34.7	34.7	38.7
Luis	0300	5 Sep	60.7	7.0	53.3	53.2	56.7
Luis	1700	5 Sep	50.7	6.4	50.3	50.2	53.9
Marilyn	0438	16 Sep	46.8	5.3	44.5	44.5	48.3
Opal	1200	4 Oct	60.4	9.1	63.2	63.0	66.0
Opal	2140	4 Oct	46.0	6.8	52.4	52.2	55.8
Roxanne	0000	11 Oct	48.1	5.2	44.0	43.9	47.8

respectively. Although a much larger dataset would be required to note a consistent bias, Table 2 shows that PW relationships underestimated V_{ms} in several 1995 landfalling storms and should therefore be used with caution. HRD analysis winds were stronger in Erin, Luis at 0300 UTC, Opal at 1200 UTC, and Roxanne; weaker in Opal at 2140 UTC; and nearly the same in Luis at 1700 UTC and Marilyn.

The history and limitations of PW relationship usage have discussed by Black (1993) and Willoughby (1995). Limitations of PW relationships are associated with failure to properly account for multiple wind maxima and a sensitivity to the shape of the profile of velocity as a function of radius. The Opal landfall analysis suggests that PW relationships may have additional limitations when used on tropical cyclones with strongly sheared flow caused by interaction with midlatitude systems or cooler water areas in northern latitudes.

6. Conclusions

The wind fields of the most significant landfalling tropical cyclones in the Atlantic basin of 1995 have been documented. The winds discussed in this paper were associated with intensifying (Marilyn, Erin, Roxanne), weakening (Opal), and near steady-state (Luis) storms that produced insured losses totaling nearly $8 billion. Much damage can be attributed to interactions of the wind with topography or sea surface response to wind stress leading to storm surge and waves. In addition to 86 real-time analyses conducted by HRD in 1995 storms, Hurricanes Erin and Opal were subject to further analysis after obtaining additional post-storm data.

Hurricane Opal was affected by a shearing flow and dry air associated with a midlatitude trough and cold front. These factors combined to produce a very asymmetric wind field with winds at the surface stronger than flight level on the weak west side of the storm. Near-neutral air–sea temperature differences and a decreased coverage of eyewall convection on the east side of the storm caused relatively weak winds compared to those estimated from pressure–wind relationships. The Opal

wind analyses highlight the complexity that results when a hurricane encounters rapidly changing synoptic conditions. Influences like the interaction with a midlatitude jet can make it difficult to interpret flight-level observations and simple wind models based on pressure–wind relationships or rotation-plus-translation do not address such complexity. The best solution is to actually measure the quantity we are trying to predict. For hurricanes over water this means hastening the transfer of remote surface wind sensing capabilities from research to operations and enhancing the NDBC buoy (including drifting buoys) and C-MAN network. Over land, this means improving the survivability and accessibility of high quality surface wind observations.

In contrast, Hurricane Erin was strengthening before its second landfall in Florida's panhandle; Erin was slightly weaker in wind strength but much better organized convectively. Wind fields shown here for Hurricane Marilyn are a product of poststorm analysis but are very similar to those produced in real time; analyses shown for Hurricanes Luis and Roxanne are identical to those transmitted to NHC forecasters for evaluation. Hurricanes Marilyn and Luis affected islands with complex terrain where several reports compared favorably with HRD analyses but a couple of unconfirmed reports contained winds in excess of the analyses. Such reports may be valid if speedup affects predicted by boundary layer wind tunnel model studies are applicable to hurricanes; experiments with mesoscale models could potentially assess locations with complex terrain that are susceptible to wind speedup affects. Wind measurements on island ridges and hilltops are needed to validate speedup estimates.

Emergency management lead time estimates were made for all storms assuming that preparations needed to be complete by the time of gale force wind onset. Lead times ranged from as low as 0 h (for Roxanne at Cozumel), to 10 h (Luis at Barbuda and Antigua), to as high as 19.5 h (Marilyn at St. Thomas). The lack of lead time (based on issuance of a hurricane warning) at Cozumel for Hurricane Roxanne underscores the importance of promoting storm preparation activities while under a tropical storm warning or hurricane watch because of storm intensification uncertainty.

High-resolution wind measurements are critical for reconstructing the wind fields of landfalling hurricanes. These data are also important for establishing the extreme wind climatology of a location. This climatology guides Monte Carlo simulations that construct extreme wind frequency distributions that determine design winds and wind loading criteria in local building codes. These codes govern building designs and construction practices that establish the level of safety to lives and property. Typically, the codes describe building practices that will allow sufficient wind load resistance for a structure to resist wind speeds with an annual exceedance probability of 2%. In other words the current codes specify that buildings survive extreme wind loads

that may occur with a mean return period of 50 years. The current ASOS wind measurement system has limitations that affect many user groups (Powell 1993). If the ASOS wind instruments fail to sample the entire storm, or sample it in a way that is incompatible with past wind records, the climatology will underestimate the true risk leading to a weak building code that may jeopardize life and property. Unfortunately, noncommissioned ASOS stations in Destin, Florida; St. Thomas, U.S. Virgin Islands; and St. Croix, U.S. Virgin Islands, experienced power losses that prevented complete data archival. ASOS systems need to be retrofitted to allow for supplemental power and threshold-activated storage of high-resolution wind measurements and sea level pressure.

REFERENCES

ASCE, 1995: Minimum design loads for buildings and other structures. ASCE 7-95, American Society of Civil Engineers, 134 pp. [Available from American Society of Civil Engineers, New York, NY 10017.]

Associated Press, 1995: Hurricane survivors recount 35 scary hours. *New York Times,* Late Edition, 19 October, Section: A, Foreign Desk, 5.

Atkinson, G. D., and C. R. Holliday, 1977: Tropical cyclone minimum sea level pressure/maximum sustained wind relationship for the western North Pacific. *Mon. Wea. Rev.,* **105,** 421–427.

Black, P. G., 1993: Evolution of maximum wind estimates in ty-

phoons. *Proc. ICSU/WMO Int. Symp. on Tropical Cyclone Disasters,* Beijing, China, Peking University Press, 104–115.

Bradley, E. P., 1980: An experimental study of the profiles of wind speed, shearing stress, and turbulence characteristics close to the ground over various escarpment shapes. *Bound.-Layer Meteor.,* **106,** 101–123.

Burpee, R. W., and Coauthors, 1994: Real-time guidance provided by NOAA's Hurricane Research Division to forecasters during Emily of 1993. *Bull. Amer. Meteor. Soc.,* **75,** 1765–1783.

Caribbean Uniform Building Code, 1989: Part 2—Structural design requirement. Georgetown, Guyana: Caribbean Community Secretariat, 55 pp.

DeMaria, M., S. M. Aberson, K. V. Ooyama, and S. J. Lord, 1992: A nested spectral model for hurricane track forecasting. *Mon. Wea. Rev.,* **120,** 1628–1643.

Dvorak, V. F., 1984: Tropical cyclone intensity analysis using satellite data. NOAA Tech. Rep. NESDIS 11, 47 pp. [Available from U.S. Dept. of Commerce, Washington, DC 20233.]

Fujita, T. T., 1971: Proposed characterization of tornados and hurricanes by area and intensity. SMRP Res. Paper No. 91, Dept. of Geophys. Sci., University of Chicago, 42 pp. [Available from Dept. of Geophys. Sciences, University of Chicago, 5734 Ellis Avenue, Chicago, IL 60637.]

——, 1993: Wind fields of Andrew, Omar, and Iniki, 1992. Preprints, *20th Conf. on Hurricanes and Tropical Meteorology,* San Antonio, TX, Amer. Meteor. Soc., 46–49.

Glanville, M. J., and K. C. S. Kwok, 1998: Measurements of topographic multipliers and flow separation from a steep escarpment. Part II: Model measurements. *J. Wind Engin. Ind. Aerodyn.,* in press.

Holmes, J. D., R. W. Banks, and P. Paevere, 1998: Measurements of topographic multipliers and flow separation from a steep escarpment. Part I: Full scale measurements. *J. Wind. Engin. Ind. Aerodyn.,* in press.

Husty, D., 1995: What hit us? 130 mph winds, expert says. *The Virgin Island Daily News,* 16 October.

Jackson, P. S., and J. C. R. Hunt, 1975: Turbulent wind flow over a low hill. *Quart. J. Roy. Meteor. Soc.,* **101,** 929–955.

Jensen, N. O., and E. W. Peterson, 1978: On the escarpment wind profile. *Quart. J. Roy. Meteor. Soc.,* **104,** 719–728.

Lawrence, M., M. Mayfield, L. Avila, R. Pasch, and E. Rappaport, 1998: Atlantic hurricane season of 1995 *Mon. Wea. Rev.,* **126,** 1124–1151.

Lohr, L., 1995: St. Johnians remain calm, begin picking up. *The Virgin Island Daily News,* 18 September.

Lord, S. J., and J. L. Franklin, 1987: The environment of Hurricane Debby. Part I: Winds. *Mon. Wea. Rev.,* **115,** 2760–2780.

Marshall, R. D., and J. L. Schroeder, 1997: Hurricane Marilyn in the Caribbean—Measured wind speeds and design wind speeds compared. NISTIR 5987. [Available from National Institute for Standards and Technology, Building and Fire Research Laboratory, Gaithersburg, MD 20899.]

Means, B., T. A. Reinhold, and D. C. Perry, 1996: Wind loads for low rise buildings on escarpments. *Structures Congress XIV,* Chicago, IL, American Society of Civil Engineers, 1045–1052.

National Research Council, 1994: Hurricane Hugo. Puerto Rico, the Virgin islands, and Charleston, South Carolina. *Natural Disaster Studies.* Vol. 6, 276 pp.

Ooyama, K. V., 1987: Scale controlled objective analysis. *Mon. Wea. Rev.,* **115,** 2479–2506.

Powell, M. D., 1980: Evaluations of diagnostic marine boundary layer models applied to hurricanes. *Mon. Wea. Rev.,* **108,** 757–766.

——, 1993: Wind measurement and archival under the Automated Surface Observing System (ASOS): User concerns and opportunity for improvement. *Bull. Amer. Meteor. Soc.,* **74,** 615–623.

——, and S. H. Houston, 1996: Hurricane Andrew's landfall in south Florida. Part II: Surface wind fields and potential real-time applications. *Wea. Forecasting,* **11,** 329–349.

——, P. P. Dodge, and M. L. Black, 1991: The landfall of Hurricane

Hugo in the Carolinas: Surface wind distribution. *Wea. Forecasting,* **6,** 379–399.

——, S. H. Houston, and T. Reinhold, 1996: Hurricane Andrew's landfall in south Florida. Part I: Standardizing measurements for documentation of surface wind fields. *Wea. Forecasting,* **11,** 304–328.

Roux, F., and F. D. Marks, 1996: Extended velocity track display (EVTD): An improved processing method for Doppler radar observation of tropical cyclones. *J. Atmos. Oceanic Technol.,* **13,** 875–899.

Saffir, H. S., 1977: Design and construction requirements for hurricane resistant construction. Preprint No. 2830, ASCE, 20 pp. [Available from American Society of Civil Engineers, New York, NY 10017.]

Simpson, R. H., and H. Riehl, 1981: *The Hurricane and its Impact.* Louisiana State University Press, 398 pp.

Standards Australia, 1989: SAA loading code. Part 2: Wind loads. AS1170.2-1989, Standards Australia, 96 pp. [Available from Standards Australia, Standards House, 80 Arthur Street, North Sydney, New South Wales, Australia.]

Wernly, D., 1996: Hurricane Marilyn September 15–16, 1995. Natural Disaster Survey Report. National Weather Service. [Available from National Weather Service, Office of Meteorology, 1325 East-West Highway, Room 14370, Silver Spring, MD 20910.]

Willoughby, H. E., 1995: Mature structure and evolution. Global perspectives on tropical cyclones. WMO/TD-No. 693, Tropical Cyclone Programme Report No. TCP-38, 21–62. [Available from the World Meteorological Organization, Case Postale 2300, CH-1211 Geneva 2, Switzerland.]

——, J. A. Clos, and M. G. Shoreibah, 1982: Concentric eye walls, secondary wind maxima, and the evolution of the hurricane vortex. *J. Atmos. Sci.,* **39,** 395–411.